

Catalytic Mechanism of Galactose Oxidase: A Theoretical Study

Fahmi Himo,^{*,†} Leif A. Eriksson,[‡] Feliu Maseras,[§] and Per E. M. Siegbahn[†]

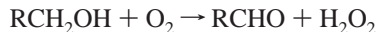
Contribution from the Department of Physics, Stockholm University, Box 6730, S-113 85 Stockholm, Sweden, Department of Quantum Chemistry, Uppsala University, Box 518, 751 20 Uppsala, Sweden, and Unitat de Química Física, Universitat Autònoma de Barcelona, E-08193 Bellaterra, Catalonia, Spain

Received December 30, 1999. Revised Manuscript Received May 1, 2000

Abstract: Density functional methods, alone and together with molecular mechanics, are used to study the catalytic mechanism of galactose oxidase. This enzyme catalyzes the conversion of primary alcohols to the corresponding aldehydes, coupled with reduction of dioxygen to hydrogen peroxide. It is shown that the proposed mechanism for this enzyme is energetically feasible. In particular the barrier for the postulated rate-limiting hydrogen atom transfer between the substrate and the tyrosyl radical, located at equatorial Tyr272, is very plausible. We propose that the radical site, prior to the initial proton transfer step, is located at the axial tyrosine (Tyr495). The radical is transferred to the equatorial tyrosine (Tyr272) simultaneously with the proton transfer. It is, furthermore, argued that the electron transfer from the ketyl radical intermediate to Cu(II) cannot be very exothermic, because this would render the oxygen reduction steps rate-limiting. Finally, the cysteine cross-link on the active site tyrosine is shown to have very minor effects on the energetics of the reaction.

I. Introduction

Galactose oxidase (GO) is a mononuclear copper enzyme that catalyzes the two-electron oxidation of a large number of primary alcohols to their corresponding aldehydes, coupled with the reduction of dioxygen to hydrogen peroxide:¹



The protein is a single polypeptide with molecular mass of ca. 68 500. In addition to the copper center, the enzyme utilizes a protein radical cofactor, which has been assigned to the Tyr272 residue. GO can exist in three distinct oxidation states: the highest state with Cu(II) and tyrosyl radical, the intermediate state with Cu(II) and tyrosine, and the lowest state with Cu(I) and tyrosine. The highest oxidation state is the catalytically active one. The protein radical interacts antiferromagnetically with the copper ion, resulting in an EPR silent species.

The crystal structure of the active form of GO has been determined at pH 4.5 and 7.0. The copper site was found to be close to the surface with essentially square-pyramidal coordination with Tyr495 in an axial position and Tyr272, His581, His496, and a water or acetate, to be replaced by substrate, in equatorial positions (Figure 1). Tyr272 (the radical site) is cross-linked to a cysteine residue (Cys228) through a thioether bond at the ortho position to the phenol OH.² The Tyr-Cys moiety is, moreover, π -stacked to a tryptophan residue (Trp290), which also controls entry to the active site. Another interesting feature

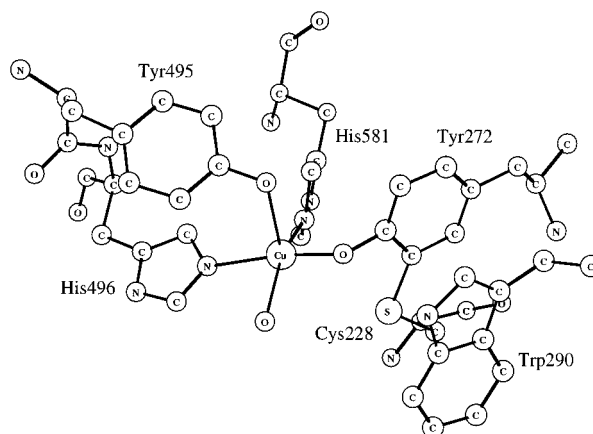


Figure 1. Crystal structure of the active site of galactose oxidase. The substrate is believed to replace the exogenous water in the equatorial position.

of the active site is the direct backbone link between axial Tyr495 and equatorial His496.

On the basis of extensive spectroscopic work and also on the crystal structure, a mechanism has been proposed for GO (Scheme 1).³ In this mechanism, after the substrate binds to the equatorial copper position (occupied by water or acetate in the crystal structures), the first step is a proton transfer from the alcohol to the axial tyrosinate (Tyr495). Next, in a step known from isotope substitution experiments to be at least partially rate-limiting and probably the major rate-limiting step, a hydrogen atom is transferred from the substrate to the equatorial modified tyrosyl radical (Tyr272). The resulting substrate derived ketyl radical is then oxidized through electron transfer to the copper center yielding Cu(I) and aldehyde

* Corresponding author. E-mail: himo@physto.se. Fax: +46-8-347817.

[†] Stockholm University.

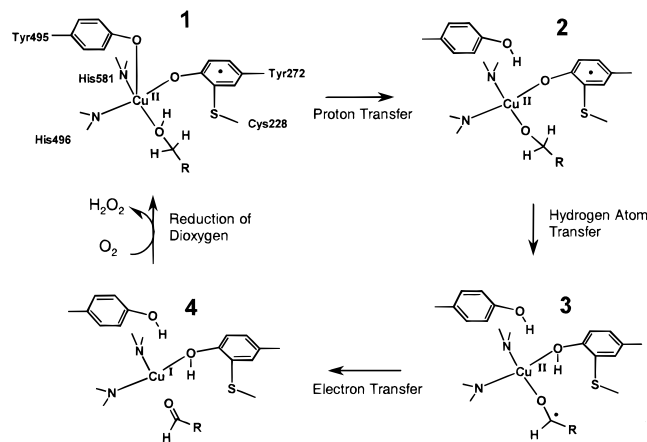
[‡] Uppsala University.

[§] Universitat Autònoma de Barcelona.

(1) Recent reviews: (a) Stubbe, J.-A.; van der Donk, W. *Chem. Rev.* **1998**, 98, 705. (b) Klinman, J. P. *Chem. Rev.* **1996**, 96, 2541. (c) Whittaker, J. W. In *Metal Ions in Biological Systems*; Vol. 30, Metalloenzymes Involving Amino Acid-Residue and Related Radicals; Sigel, H., Sigel, A., Eds.; Marcel Dekker: New York, 1994; p 315.

(2) Ito, N.; Phillips, S. E. V.; Stevens, C.; Ogel, Z. B.; McPherson, M. J.; Keen, J. N.; Yadav, K. D. S.; Knowles, P. F. *Nature* **1991**, 350, 87.

(3) (a) Whittaker, M. M.; Whittaker, J. W. *J. Biol. Chem.* **1988**, 263, 6074. (b) Branchaud, B. P.; Montague-Smith, M. P.; Kosman, D. J.; McLaren, F. R. *J. Am. Chem. Soc.* **1993**, 115, 798. (c) Whittaker, M. M.; Whittaker, J. W. *Biophys. J.* **1993**, 64, 762.

Scheme 1. Reaction Mechanism Previously Proposed for Galactose Oxidase³

product. On the basis of experiments with various inhibitors, Branchaud and co-workers have suggested that the two latter steps occur simultaneously in a concerted manner.⁴ Cu(I) and tyrosine are, finally, reoxidized by molecular oxygen, regenerating Cu(II) and tyrosyl, and giving hydrogen peroxide product.

Large efforts have been made to synthesize biomimetic models of the active site of galactose oxidase.⁵ Some of these studies have recently managed to reproduce the characteristic features of the GO active site, with respect to its structural, spectroscopic, and also catalytic reactivity properties.

Recently, Wachter and Branchaud⁶ presented a semiquantitative energy profile for the reaction steps of GO using available experimental data on GO and relevant model systems. The main hypothesis in that work was that protein rigidity in GO maintains a distorted square-planar geometry which is better for Cu(II) than Cu(I), reducing hence the copper potential (estimated to be between -0.3 and -0.5 V).

(4) (a) Wachter, R. M.; Branchaud, B. P. *J. Am. Chem. Soc.* **1996**, *118*, 2782. (b) Wachter, R. M.; Branchaud, B. P. *Biochemistry* **1996**, *35*, 14425. (c) Wachter, R. M.; Montague-Smith, M. P.; Branchaud, B. P. *J. Am. Chem. Soc.* **1997**, *119*, 7743.

(5) (a) Wang, Y.; Stack, T. D. P. *J. Am. Chem. Soc.* **1996**, *118*, 13097. (b) Wang, Y.; DuBois, J. L.; Hedman, B.; Hodgson, K. O.; Stack, T. D. P. *Science* **1998**, *279*, 537. (c) Whittaker, M. M.; Chuang, Y.-Y.; Whittaker, J. W. *J. Am. Chem. Soc.* **1993**, *115*, 10029. (d) Whittaker, M. M.; Duncan, W. R.; Whittaker, J. W. *Inorg. Chem.* **1996**, *35*, 382. (e) Halfen, J. A.; Young, V. G.; Tolman, W. B. *Angew. Chem., Int. Ed. Engl.* **1996**, *35*, 1687. (f) Halfen, J. A.; Jazdzewski, B. A.; Mahapatra, S.; Berreau, L. M.; Wilkinson, E. C.; Que, L.; Tolman, W. B. *J. Am. Chem. Soc.* **1997**, *119*, 8217. (g) Jazdzewski, B. A.; Young, V. G.; Tolman, W. B. *Chem. Commun.* **1998**, 2521. (h) Müller, J.; Weyhermüller, T.; Bill, E.; Hildebrandt, P.; Ould-Moussa, L.; Glaser, T.; Wieghardt, K. *Angew. Chem., Int. Ed. Engl.* **1998**, *37*, 616. (i) Chaudhuri, P.; Hess, M.; Müller, J.; Hildenbrand, K.; Bill, E.; Weyhermüller, T.; Wieghardt, K. *J. Am. Chem. Soc.* **1999**, *121*, 9599. (j) Itoh, S.; Takayama, S.; Arakawa, R.; Furuta, A.; Komatsu, M.; Ishida, A.; Takamuku, S.; Fukuzumi, S. *Inorg. Chem.* **1997**, *36*, 1407. (k) Itoh, S.; Taki, M.; Takayama, S.; Nagatomo, S.; Kitagawa, T.; Sakurada, N.; Arakawa, R.; Fukuzumi, S. *Angew. Chem., Int. Ed. Engl.* **1999**, *38*, 2774. (l) Pierpont, C. G.; Ruf, M. *Angew. Chem., Int. Ed. Engl.* **1998**, *37*, 1736. (m) Adams, H.; Bailey, N. A.; Campbell, I. K.; Fenton, D. E.; He, Q. Y. *J. Chem. Soc., Dalton Trans.* **1996**, 2233. (n) Adams, H.; Bailey, N. A.; Fenton, D. E.; He, Q. Y.; Ohba, M.; Okawa, H. *Inorg. Chim. Acta* **1994**, *215*, 1. (o) Vaidyanathan, M.; Viswanathan, R.; Palaniandavar, M.; Balasubramanian, T.; Prabhakaran, P.; Muthiah, T. P. *Inorg. Chem.* **1998**, *37*, 6418. (p) Zurita, D.; Scheer, C.; Pierre, J.-L.; Saint-Aman, E. *J. Chem. Soc., Dalton Trans.* **1996**, 4331. (q) Halcrow, M. A.; Chia, L. M. L.; Liu, X.; McInnes, E. J. L.; Yellowlees, L. J.; Mabbs, F. E.; Davies, J. E. *Chem. Commun.* **1998**, 2465. (r) Sokolowski, A.; Leutbecher, H.; Weyhermüller, T.; Schnepf, R.; Bothe, E.; Bill, E.; Hildebrandt, P.; Wieghardt, K. *J. Biol. Inorg. Chem.* **1997**, *2*, 444. (s) Zurita, D.; Menage, S.; Pierre, J.-L.; Saint-Aman, E. *New J. Chem.* **1997**, *21*, 1001. (t) Zurita, D.; Gautier-Luneau, L.; Menage, S.; Pierre, J.-L.; Saint-Aman, E. *J. Biol. Inorg. Chem.* **1997**, *2*, 46.

(6) Wachter, R. M.; Branchaud, B. P. *Biochim. Biophys. Acta* **1998**, *1384*, 43.

In the present work, we have examined the catalytic mechanism of galactose oxidase using the density functional theory (DFT) functional B3LYP.⁷ This method, developed by Becke, includes three parameters fitted to experimental atomization energies, ionization potentials, and electron affinities, and has proven to be very suitable for this kind of study.⁸

The backbone link between Tyr495 and His496 was added using the IMOMM (Integrated Molecular Orbital/Molecular Mechanics) hybrid method.⁹ This method uses quantum mechanics and molecular mechanics descriptions for different parts of the system, and it has proven to be successful in the quantification of steric effects in a number of organometallic applications.¹⁰

II. Computational Details

The pure density functional theory calculations reported in the present study were carried out using the functional B3LYP,⁷ as implemented in the Gaussian94 program package.¹¹ Geometries were optimized with the double- ζ basis set LANL2DZ. On the basis of these geometries, more accurate energies were calculated with a large basis set, including polarization and diffuse functions. Zero-point vibrational energy correction for the hydrogen atom transfer step was calculated at the same level as the geometry optimization. For the other steps, preliminary tests showed that the ZPE effects are small and were thus not calculated. All the spin populations reported here are calculated using Mulliken population analysis.

The IMOMM calculations were performed with a program built from modified versions of the standard programs Gaussian92/DFT¹² for the quantum mechanics (QM) part, and MM3(92)¹³ for the molecular mechanics (MM) part. The method used in the QM part is the same as the one used in the pure DFT calculations, B3LYP/LANL2DZ for the geometry optimization and the same large basis set for the energy calculation. All geometrical parameters were optimized, except the bond distances connecting the QM and the MM part, which were kept constant: C–H (1.101 Å) in the ab initio part and C–C (1.434 Å) in the molecular mechanics part. The van der Waals radius for Cu was taken from the UFF force field. The full details of the IMOMM method are describe elsewhere.⁹

As mentioned in the Introduction, the unpaired electrons of the tyrosyl radical and the copper atom couple antiferromagnetically. The correct electronic state is hence the open shell singlet. Owing to the single determinant nature of the DFT method, there will be some errors in the description of this state. These errors can be corrected for by calculating the triplet energies and using Landé's interval rule.¹⁴ However, the spin populations obtained are not integers (rather around 0.6) making this procedure not fully applicable. Tests showed that the corrections are typically in the order of a few kilocalories per mole, which will not change any of the conclusions drawn in the present work about the mechanism of GO.

III. Results and Discussion

Before discussing the results of our calculations it is important to note a simple but crucial fact. From experimental heats of

(7) (a) Lee, C.; Yang, W.; Parr, R. G. *Phys. Rev.* **1988**, *B37*, 785. (b) Becke, A. D. *J. Chem. Phys.* **1993**, *98*, 1372. (c) Becke, A. D. *J. Chem. Phys.* **1993**, *98*, 5648.

(8) (a) Siegbahn, P. E. M. *Inorg. Chem.* **1999**, *38*, 2880. (b) Siegbahn, P. E. M.; Crabtree, R. H. *J. Am. Chem. Soc.* **1999**, *121*, 117. (c) Wirstam, M.; Blomberg, M. R. A.; Siegbahn, P. E. M. *J. Am. Chem. Soc.* **1999**, *121*, 10178.

(9) Maseras, F.; Morokuma, K. *J. Comput. Chem.* **1995**, *16*, 1170.

(10) (a) Maseras, F. *Top. Organomet. Chem.* **1999**, *4*, 165. (b) Ujaque, G.; Maseras, F.; Lledos, A. *J. Am. Chem. Soc.* **1999**, *121*, 1317. (c) Maseras, F.; Eisenstein, O. *New J. Chem.* **1998**, *22*, 5.

(11) Frisch, M. J. et al. *Gaussian 94, Revision B.2*; Gaussian Inc.: Pittsburgh, PA, 1995.

(12) Frisch, M. J. et al. *Gaussian 92/DFT*; Gaussian Inc.: Pittsburgh, PA, 1993.

(13) Allinger, N. L. *mm3(92)*; QCPE: Bloomington, IN, 1992.

(14) Noodleman, L.; Case, D. A. *Adv. Inorg. Chem.* **1992**, *38*, 423.

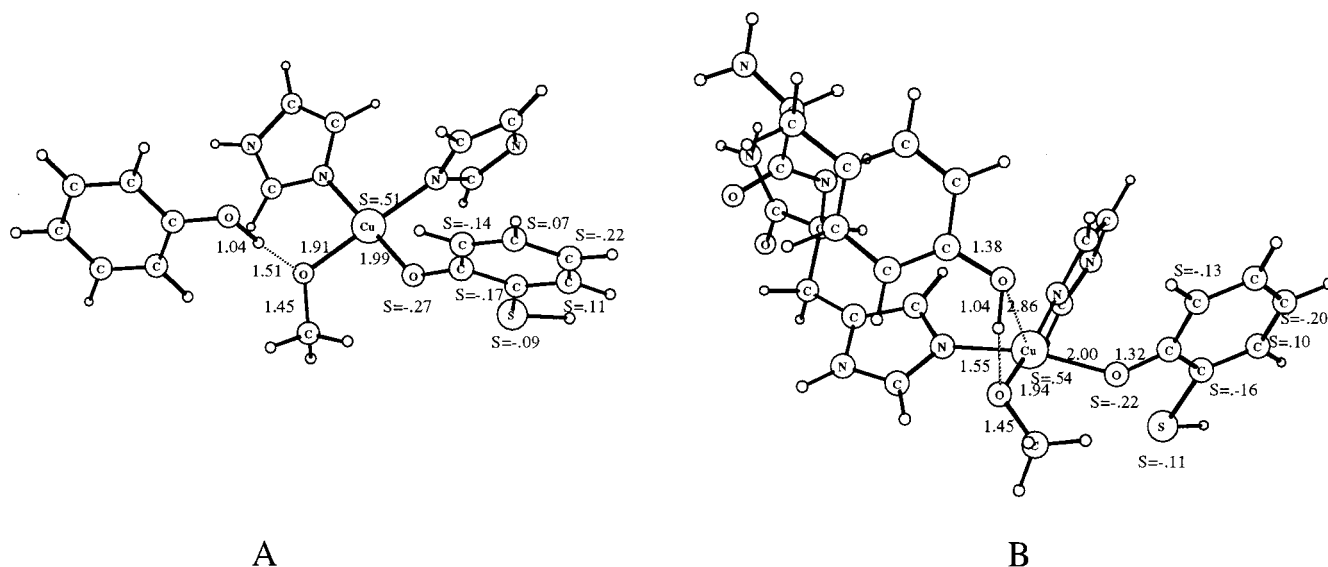
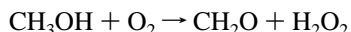


Figure 2. Optimized structure of the system after proton transfer (structure 2 in Scheme 1) calculated with (A) B3LYP and (B) IMOMM(B3LYP)/MM3). Mulliken spin populations in selected atoms are included.

formation one can calculate that the net reaction catalyzed by galactose oxidase (with methanol as substrate):



is exothermic by 10.7 kcal/mol¹⁵ (in our calculations 6.7 kcal/mol). The fact that the reaction is catalyzed by the enzyme does not change this total exothermicity. This now sets some restrictions on the energetics involved in the catalyzed reaction. For instance, the proposed electron transfer from the ketyl radical anion to the Cu(II) center cannot be very exothermic, since this would render the oxygen reduction steps rate-limiting, with a barrier higher than the estimated 14 kcal/mol. The discrepancy between experimental and calculated exothermicities (10.7 vs 6.7 kcal/mol) originates most likely from an overbound O₂ species in the DFT calculations. In the potential energy surface presented below, we correct for that fact by simply shifting the energies upward for the steps where O₂ is free.

In what follows, we discuss first the chemical models employed in our calculations and then the catalytic mechanism step by step. The effects of the cysteine cross-link on the energetics of the reaction will also be discussed.

(a) Chemical Models. At the level of theory used in the present work it is essential to use as small models as possible of the active site to limit the computational time. At the same time, one has to ensure that the basic chemical features of the system are kept intact. In our calculations, the four equatorial ligands (two histidines, one modified tyrosine, and substrate alcohol) and the axial tyrosine ligand were included. In the pure DFT calculations, the histidines were modeled by imidazoles. The equatorial tyrosine was modeled by SH-substituted phenol, whereas the somewhat smaller, but fully adequate, vinyl alcohol served as a model for the axial tyrosine. As substrate we used the simplest alcohol, methanol. In the IMOMM calculations, the quantum part was identical to the pure QM model. The MM part consisted of the rest of the axial tyrosine residue (Tyr495) and the protein backbone link between it and the equatorial histidine (His496). We have chosen to limit the MM part of the model to include only this backbone link to isolate the effects of that.

Another modeling point that needs to be mentioned is that we use a charge neutral model for the complex. This approach has previously been applied successfully to a number of

organometallic and bioinorganic systems.¹⁶ Also for bioorganic systems the approach has proven to be successful, as, for instance, in the studies of the catalytic mechanisms of pyruvate formate-lyase¹⁷ and the substrate reaction of aerobic ribonucleotide reductase.¹⁸ In the present work, the choice of neutral model implies that one of the histidine ligands needs to be deprotonated to obtain a correct oxidation state of the copper atom.

(b) Proton Transfer. The first step in the proposed mechanism is a proton transfer (PT) from the substrate to the axial tyrosine. This step was by Wachter and Branchaud estimated to be isothermic and very fast.⁶ Docking a galactose substrate to the enzyme using molecular modeling techniques indicated that a hydrogen bond is formed between the alcoholic oxygen and the phenolic oxygen of the axial Tyr495 upon substrate binding (1).¹⁹

In our calculations, the PT reaction occurs without barrier in the pure DFT calculations. In fact, when trying to optimize the geometry of the complex with alcohol coordinating to copper, the proton moves over automatically during the course of the optimization from the substrate alcohol to the axial tyrosine. The axial tyrosine then completely dissociates from the copper and moves to form a hydrogen bond to the oxygen of the substrate alcoholate (Figure 2a).

A stable minimum with the proton still on the substrate could, however, be optimized when introducing the backbone link between Tyr495 and His496 in the IMOMM calculations (Figure 3). Although the protein backbone sets steric limitations to the degree of movement of the Tyr495, this residue is found also here to dissociate from the copper and form a hydrogen bond to the substrate upon protonation. Acid titration experiments support that the ligand dissociates upon receiving a proton from the substrate.²⁰

(15) Curtiss, L. A.; Krishnan, R.; Trucks, G. W.; Pople, J. A. *J. Chem. Phys.* **1991**, *94*, 7221.

(16) (a) Siegbahn, P. E. M. *J. Am. Chem. Soc.* **1995**, *117*, 5409. (b) Pavlov, M.; Siegbahn, P. E. M.; Blomberg, M. R. A.; Crabtree, R. H. *J. Am. Chem. Soc.* **1998**, *120*, 548. (c) Siegbahn, P. E. M.; Crabtree, R. H. *J. Am. Chem. Soc.* **1997**, *118*, 3103. (d) Lind, T.; Siegbahn, P. E. M.; Crabtree, R. H. *J. Phys. Chem. B* **1999**, *103*, 1193.

(17) Himo, F.; Eriksson, L. A. *J. Am. Chem. Soc.* **1998**, *120*, 11449.

(18) Siegbahn, P. E. M. *J. Am. Chem. Soc.* **1998**, *120*, 8417.

(19) Wachter, R. M.; Branchaud, B. P. *J. Am. Chem. Soc.* **1996**, *118*, 2782.

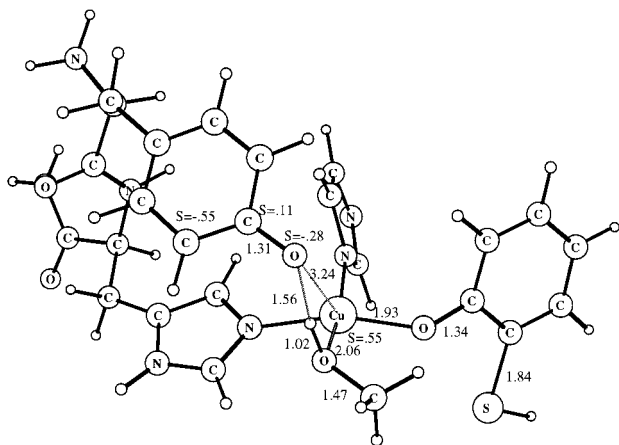


Figure 3. IMOMM(B3LYP/MM3) optimized structure of the system prior to the proton transfer (structure **1** in Scheme 1).

In IMOMM, the proton-transfer step (**1** → **2**) is exothermic by 3.2 kcal/mol. In the pure DFT model, the exothermicity of the reaction can be estimated by freezing the O–H distance in the alcohol and optimizing all other degrees of freedom. Doing this, we find the reaction to be exothermic by 3.8 kcal/mol. This shows that the large movement of Tyr495 in the pure DFT calculation is not associated with a large energy gain. The transition state for the proton transfer could not be optimized. However, by moving the proton in steps, the barrier was estimated to be less than 3 kcal/mol, confirming that the reaction is very fast.

An interesting result that comes out from the calculations is that the radical site prior to the proton transfer (**1**) is not the equatorial cysteine-substituted tyrosine residue, but rather the axial tyrosine (Figure 3). The axial position is the weakest one in the square-pyramidal coordination of Cu(II), and thus the most natural place for the radical to be in. To make sure that this result is not an effect of the models used (phenol equatorially and vinyl alcohol axially), we performed a larger calculation with phenols in both positions. The result was the same. We have also done a series of model calculations²¹ with different ligands, from simple hydroxyls and waters to full phenols and imidazoles. All the calculations are consistent in having the radical located axially, when both axial and equatorial ligands (phenols or models of phenols) are unprotonated, which is the situation in the enzyme before the proton is transferred from the substrate to the axial tyrosine. Also when adding a sulfur substituent to the equatorial phenol, the radical was located at the axial, nonsubstituted phenol.

Stack and co-workers^{5a,b} have managed to synthesize model complexes that resemble both the spectroscopic characteristics and the catalytic activity of galactose oxidase. The ligands were chosen to force the copper to adopt non-square-planar coordination with one of the phenols being axial, mimicking the copper coordination in the enzyme. For these complexes, EXAFS and edge XAS experiments show that the radical is most likely located on the axial phenol. Recent calculations by Rothlisberger and Carloni²² on these model systems confirm this fact.

In our calculations, after the proton transfer (**2**), the radical is located at the equatorial tyrosine 272 (Figure 2), inferring that simultaneously with the proton transfer an electron is moved from the equatorial tyrosine to the axial one.

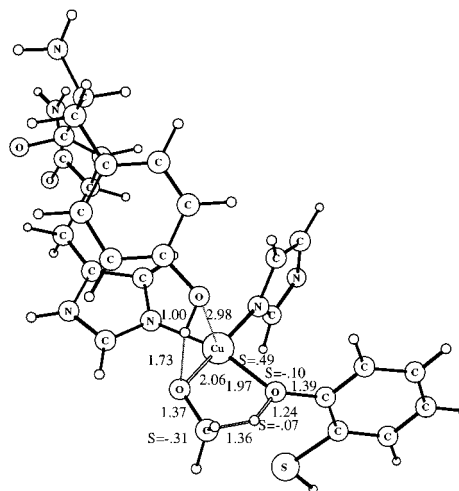


Figure 4. IMOMM(B3LYP/MM3) optimized geometry of the transition state for the proposed rate-limiting hydrogen atom transfer.

Stack's model systems and GO active site behave, hence, very similarly, in contrast to the theory that the protein matrix is keeping the radical in the equatorial position. The difference is rather that in the model complexes of Stack, neither of the two phenolic oxygens is protonated, which makes the optimal radical site remain in the weak axial position. The substrate used in the model compounds is alcoholate (⁻OCH₃), which, in contrast to the GO substrate, cannot give a proton to the axial phenol and thereby move the radical site to the equatorial tyrosine.

It should here be remarked that the major difficulty in assigning the radical site arises from the fact that the active form of GO is EPR-silent. Accordingly, the identification of Tyr272 as the radical site was made for the EPR-active apo-enzyme, where the copper has been chelated away. The suggestion that the radical prior to the PT is located axially at Tyr495 and not at the sulfur-substituted Tyr272 is not inconsistent with that. The sulfur substitution stabilizes the tyrosyl radical by 1.7 kcal/mol (see separate section below), which is enough to localize the radical to the Tyr-Cys moiety. However, the assignment of the radical being at Tyr495 is in conflict with the interpretation of resonance Raman spectroscopy results by McGlashen et al.²⁰ Comparing the spectrum of the active form of GO with model compounds (unsubstituted and methyl- and thioether-substituted phenolates and phenoxy), the authors concluded that some of the bands arise from the thioether-substituted tyrosyl radical (Tyr272), in addition to previously identified bands from tyrosinate.²⁰

(c) Hydrogen Atom Transfer. After the deprotonation of the substrate, the next step proposed is a hydrogen atom transfer (HAT) from substrate-C2 to the Tyr272 radical (**2** → **3**). From isotope substitution experiments this step is known to be at least partially rate-limiting and probably the major rate-limiting step.

In the present study we have optimized the structure for the transition state of this hydrogen atom transfer (Figure 4). The barrier was found to be 13.6 kcal/mol in the IMOMM calculation and 11.1 kcal/mol in the pure B3LYP calculation. It is known that turnover rates of alcohols exhibit strong substituent effect.²³ For instance, galactose has a turnover number of 800 s⁻¹, while ethanol has a number of 0.02 s⁻¹. Assuming the hydrogen atom to be fully rate-determining, a barrier of ca. 14 kcal/mol can be estimated using the kinetic data for galactose as substrate.⁶ Although the calculated barrier is somewhat lower

(20) McGlashen, M. L.; Eads, D. D.; Spino, T. G.; Whittaker, J. W. *J. Phys. Chem.* **1995**, *99*, 4918.

(21) Himo, F.; Siegbahn, P. E. M. To be submitted for publication.

(22) Rothlisberger, U.; Carloni, P. *Int. J. Quantum Chem.* **1999**, *73*, 209.

(23) Wachter, R. M.; Branchaud, B. P. *Biochemistry* **1996**, *35*, 14425.

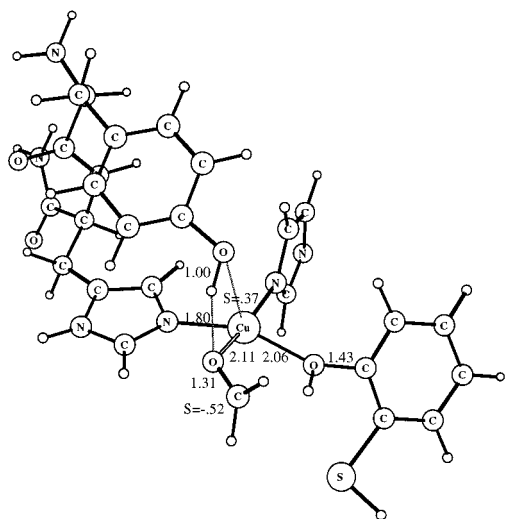


Figure 5. IMOMM(B3LYP/MM3) optimized structure of the ketyl radical intermediate (structure **3** in Scheme 1).

than the experimental estimation, it does indeed provide strong support for the proposed mechanism.

As seen in Figure 4, the critical C–H bond length is 1.36 Å in the transition state. The H–O distance is 1.24 Å. Consistently with the tyrosyl radical being a π -radical, we note that the hydrogen atom is transferred perpendicularly to the ring plane. Stretching the phenol O–H bond in the plane of the ring would lead to a high-energy σ -radical. At the transition state one spin is located at the copper ($S = 0.49$) and the other is shared by both the tyrosine and the substrate ($S = 0.15$ and 0.49 , respectively). The hydrogen atom carries 0.07 of the unpaired spin.

(d) Radical Intermediate. The hydrogen atom transfer is proposed to result in a substrate-derived ketyl radical (**3**), which then would be oxidized through electron transfer to the copper center, yielding Cu(I) and the aldehyde product (**4**). Branchaud and co-workers have raised the possibility of a concerted reaction, mainly based on experiments with radical probes.⁴

By moving from the transition state structure toward the product, we were in the present study able to localize the proposed radical intermediate in the IMOMM calculation (Figure 5). The energy of the intermediate is 4.9 kcal/mol down from the transition state, making the HAT step endothermic by 8.7 kcal/mol.

In the pure DFT calculation, all attempts to localize the ketyl radical intermediate failed, indicating that this intermediate is very unstable with the barrier for its collapse to the closed shell Cu(I) and aldehyde product being very small. In practice, this radical intermediate is therefore probably impossible to detect.

(e) Electron Transfer and Oxygen Binding. The ketyl radical intermediate (**3**) is highly unstable and will readily reduce the copper center, yielding Cu(I) and aldehyde (**4**). Wachter and Branchaud estimated this electron transfer (ET) step to be exothermic by 36 kcal/mol.⁶ In our pure QM calculations, the closed shell Cu(I) + aldehyde system (**4**) will, when optimized, have a largely distorted geometry. The two phenols dissociate to form hydrogen bonds to each other and to the aldehyde, and the angle between the two imidazoles increases from 90 to 180°. Although the backbone link between Tyr495 and His496 included in the IMOMM calculations reduces the distortion somewhat, it is clear that this species is overstabilized. It can only serve as an upper limit to the amount of energy that can be gained. The exothermicity is calculated to be around 14 kcal/mol relative to the ketyl radical intermediate. The protein matrix

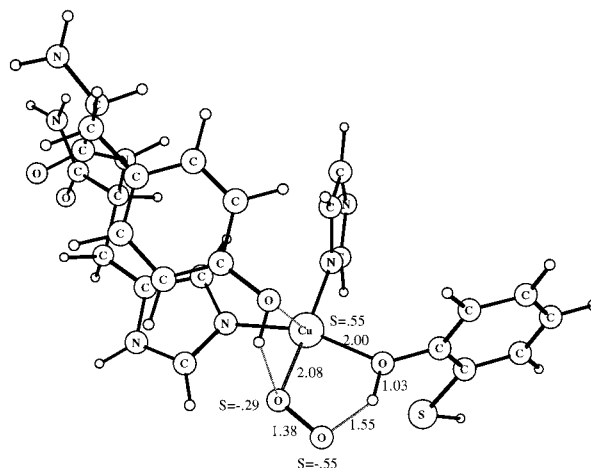


Figure 6. IMOMM(B3LYP/MM3) optimized structure of O_2^- bound to the GO active site.

will of course prevent such a large distortion and we estimate the energy of the complex, with proper coordination before the distortion, to be around 5 kcal/mol lower than the energy of the ketyl radical intermediate. This estimation is based on the energy of the system in the first few steps of the geometry optimization, i.e., before the distortion becomes very large.

Instead, energy is gained through the binding and one-electron reduction of dioxygen. Assuming release of the aldehyde product at this stage, and that dioxygen occupies its position, we find O_2^- to be bound to copper by 20.6 kcal/mol more than the substrate alcoholate ($^- \text{OCH}_3$). The structure is shown in Figure 6.

The calculated energy of this state is quite reasonable. As mentioned before, the overall cycle is only exothermic by ca. 11 kcal/mol (standard enthalpies of formation). A very exothermic electron-transfer step (**3** \rightarrow **4**), leading to an energy 36 kcal/mol below the starting point (as suggested from experimental results⁶), will automatically mean that reduction of O_2 to H_2O_2 will have to be endothermic by 25 kcal/mol ($36 - 11$). This can be ruled out, being much higher than the rate-limiting hydrogen transfer step (**2** \rightarrow **3**).

(f) Role of the Cysteine Cross-link. One fundamental mechanistic question concerns the role of the thioether bond. It has been shown that the C228G mutant has 10 000 times lower activity than the wild-type enzyme, and also migrates slower on gel electrophoresis.²⁴ The three-dimensional structure did not show much change in the main chain or the copper binding site due to the mutation, except for the missing thioether bond. It was suggested that destabilization of the tyrosyl radical due to less electron delocalization caused this drop in activity.

It has also been proposed²⁵ that this thioether bond is in part responsible for the 0.5–0.6 V lowering of the oxidation potential of this species compared to normal tyrosine. However, there is now a growing body of evidence that the cysteine link only induces small perturbations in the electronic structure and energetics of the tyrosine residue. Based on a series of EPR and ENDOR experiments on both the apo-enzyme and model

(24) (a) Baron, A. J.; Stevens, C.; Wilmot, C. M.; Knowles, P. F.; Phillips, S. E. V.; McPherson, M. J. *Biochem. Soc. Trans.* **1993**, *21*, 319S. (b) McPherson, M. J.; Stevens, C.; Baron, A. J.; Ogel, Z. B.; Seneviratne, K.; Wilmot, C. M.; Ito, N.; Brocklebank, I.; Phillips, S. E. V.; Knowles, P. F. *Biochem. Soc. Trans.* **1993**, *21*, 752. (c) Baron, A. J.; Stevens, C.; Wilmot, C. M.; Seneviratne, K. D.; Blakeley, V.; Dooley, D. M.; Phillips, S. E. V.; Knowles, P. F.; McPherson, M. J. *J. Biol. Chem.* **1994**, *269*, 25095.

(25) Itoh, S.; Hirano, K.; Furuta, A.; Komatsu, M.; Ohshiro, Y.; Ishida, A.; Takamuku, S.; Kohzuma, T.; Nakamura, N.; Suzuki, S. *Chem. Lett.* **1993**, 2099.

alkylthio-substituted phenoxy radicals, it was shown by Babcock et al.²⁶ that the sulfur cross-link does not severely perturb the spin distribution of the tyrosyl radical. Comparing the spectra of methylthio-substituted radicals with unsubstituted ones, Babcock et al. detected, furthermore, no major shift in the *g*-tensors, which otherwise would be expected when heavy elements carry some of the spin in organic radicals. Recent ab initio *g*-value calculations of unsubstituted and sulfur-substituted phenoxy radicals give clear confirmation to this observation.²⁷

Using density functional calculations it was also shown that the presence of the thioether bond has very small effects on the hyperfine couplings and spin distributions.²⁸ The odd-alternant spin pattern was not perturbed, with the sulfur center only having ca. 0.12 of the unpaired spin. Further evidence was provided by electrochemical experiments. Whittaker et al.^{5c} measured the pK_a of *o*-methylthiocresol to be only 0.7 pH units lower than for unsubstituted cresol (9.5 vs 10.2). Tolman and co-workers^{5f} obtained similar results for synthetic model complexes. The $E_{1/2}$ for their model complex that has a phenol with an *o*-methylthiol substituent was shown to be only 50 mV lower than that for the same complex but with a *t*-Bu-substituent instead of the methylthiol. Finally, we have calculated the sulfur substituent effect on the O–H bond dissociation energy²⁹ of phenol. It was found that the sulfur moiety lowered the BDE by only 1.7 kcal/mol.

In the present study, we further investigated the effects of the cysteine cross-link on the potential energy surface of the GO reaction. By optimizing the geometries with and without the sulfur link, we found both the energetics and the structures to be almost identical. For instance, the barrier for the critical hydrogen atom transfer step was found to be only about 1 kcal/mol higher with the sulfur moiety compared to without. Clearly, the thioether bond has no major *electronic* effect on the tyrosine. Instead, the role of the cross-link is likely to be of structural nature.

IV. Summary and Conclusions

We have in the present work studied the catalytic mechanism of galactose oxidase by means of density functional theory. In

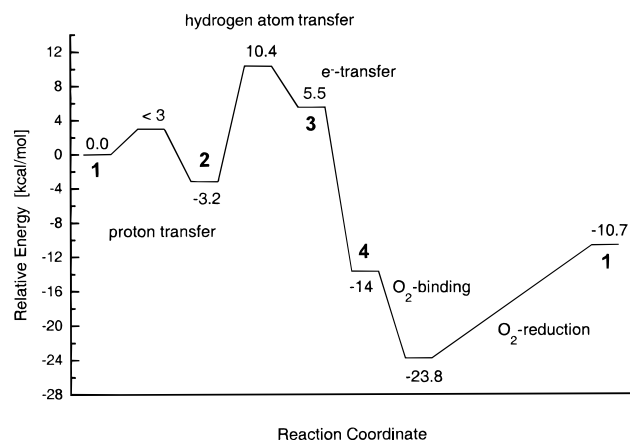
(26) Babcock, G. T.; El-Deeb, M. K.; Sandusky, P. O.; Whittaker, M. M.; Whittaker, J. W. *J. Am. Chem. Soc.* **1992**, *114*, 3727.

(27) Engström, M.; Himo, F.; Ågren, H. *Chem. Phys. Lett.* **2000**, *319*, 191.

(28) (a) Himo, F.; Babcock, G. T.; Eriksson, L. A. *Chem. Phys. Lett.* **1999**, *313*, 374. (b) Wise, E. W.; Pate, J. B.; Wheeler, R. A. *J. Phys. Chem. B* **1999**, *103*, 4772.

(29) Himo, F.; Eriksson, L. A.; Blomberg, M. R. A.; Siegbahn, P. E. M. *Int. J. Quantum Chem.* **2000**, *76*, 714.

Scheme 2. Calculated, IMOMM(B3LYP/MM3), Potential Energy Surface for the Mechanism of Galactose Oxidase



Scheme 2 we summarize the calculated energetics for the various reaction steps of the GO mechanism. The calculations strongly support the experimentally proposed mechanism, with one exception. We propose that the radical site prior to the initiating proton transfer step is located at the axial tyrosine (Tyr495) and not at the equatorial thioether-substituted Tyr272. Simultaneously with the proton-transfer step, the radical is proposed to transfer to Tyr272. We have shown that the proton-transfer step is very fast and that the rate-limiting hydrogen atom transfer step has the very feasible barrier of 13.6 kcal/mol. The proposed short-lived ketyl radical intermediate has been localized, and it was argued that the electron transfer from that to Cu(II) cannot be very exothermic. High exothermicity at that point renders the reduction of O₂ rate-limiting. Moreover, the cysteine cross-link was shown to have a very small effect on the energetics of the system.

The calculated energy profile for the catalytic reaction of GO is in full agreement with available experimental observations. However, the assignment of the radical being at axial Tyr495 prior to the proton-transfer step differs from the interpretation of resonance Raman spectra.

Acknowledgment. F.H. thanks the European Union and CESCA/CEPBA for sponsoring his stay at UAB under the "Training and Mobility of Researchers" program (Contract No. ERB FMGE CT95 0062). CESCA is also acknowledged for computer time.

JA994527R